Analysis of the Polymerization Kinetics of Homodimeric EIAV p51/51 Reverse Transcriptase Implies the Formation of a Polymerase Active Site Identical to Heterodimeric EIAV p66/51 Reverse Transcriptase†

Manfred Souquet,‡ Tobias Restle,‡ Ruth Krebs,‡ Stuart F. J. Le Grice,§ Roger S. Goody,‡ and Birgitta M. Wöhrl*,‡

Max-Planck-Institut für Molekulare Physiologie, Abteilung Physikalische Biochemie, Rheinlanddamm 201, 44139 Dortmund, Germany, and Department of Medicine, Case Western Reserve University School of Medicine, 10900 Euclid Avenue, Cleveland, Ohio 44106

Received December 23, 1997; Revised Manuscript Received April 6, 1998

ABSTRACT: Homodimeric EIAV p51/51 and heterodimeric EIAV p66/51 reverse transcriptase were purified in order to compare the different modes of DNA synthesis supported by the enzymes. Analysis of the dimerization behavior of the EIAV enzymes indicates that the dimer stability of EIAV reverse transcriptase enzymes is higher than that of their HIV-1 reverse transcriptase counterparts. EIAV p51/51 polymerizes DNA distributively whereas DNA synthesis by EIAV p66/51 is processive. Steady-state and pre-steady-state kinetic analyses of primer/template binding and nucleotide incorporation were performed with both enzymes to determine the reasons for the different polymerization behavior. Equilibrium fluorescence titrations demonstrated that the K_d values of EIAV p51/51 for binding of DNA/DNA and DNA/RNA substrates are increased 10-fold and 28-fold, respectively, as compared to EIAV p66/51. Stopped-flow measurements with DNA/DNA show that the increase in the K_d is in part due to a 17.4-fold higher dissociation rate constant (k_{-1}) for EIAV p51/51. Additionally, with EIAV p51/51, k_{diss} is increased 7-fold for DNA/DNA and 14-fold for DNA/RNA primer/template substrates, respectively. The lack of the RNase H domain in EIAV p51/51 leads to differences in the pre-steady-state kinetics of nucleotide incorporation on DNA/DNA and DNA/RNA templates. The burst of both enzymes is composed of two phases for both substrates, and the values for the corresponding pre-steady-state burst rates, k_{pol1} and k_{pol2}, are similar for both enzymes, implying the formation of identical polymerase active sites. However, the amplitudes of the two phases differ with DNA/DNA templates, indicating a different distribution between two states varying greatly in their kinetic competence.

Retroviral reverse transcriptases (RTs)[1] are multifunctional enzymes that possess RNA- and DNA-dependent DNA polymerase activities and a ribonuclease H (RNase H) activity that cleaves RNA in RNA/DNA hybrids. The RTs from closely related lentiviruses, including human immunodeficiency virus (HIV-1 and HIV-2), simian immunodeficiency virus, feline immunodeficiency virus, and equine infectious anemia virus (EIAV), show similar RT organization. They all possess a heterodimeric RT with a large (ca. 66 kDa) subunit and a small (ca. 51−58 kDa) subunit that share a common amino terminus (*1*−*5*). The small subunit lacks the carboxyl-terminal RNase H domain.

It has been shown previously for the purified recombinant wild-type HIV-1 RT p66/51 that it can be dissociated by the addition of 10−15% acetonitrile, indicating that hydrophobic interactions are necessary for dimerization. In contrast to the heterodimeric RT, the individually expressed p66 and p51 subunits of HIV-1 RT form less stable dimers. In particular, the stability of the HIV-1 p51 homodimer is very low and concentration-dependent (*6*). Since DNA polymerase and RNase H activities are exclusively associated with the dimer forms of HIV-1 RT (*6*, *7*), the individually expressed subunits are very difficult to characterize and lose polymerase activity quickly due to monomerization.

In contrast to the results obtained with HIV-1 RT, we have shown previously that the homodimeric p66 and p51 enzymes from EIAV RT form more stable dimers and can therefore be used as a model for the analysis of the polymerase activity of the homodimeric proteins (*8*). Analysis of the reaction products of EIAV p51/51 showed that it polymerizes in a distributive mode leading to very short extension products. However, heterodimeric EIAV p66/51, like HIV-1 p66/51 and the homodimeric p66 EIAV enzyme, is significantly more processive on both RNA and DNA templates (*8*−*10*). Additionally, studies with Mo-MLV RT

† This work was supported by a grant from the German Bundesministerium für Bildung, Wissenschaft, Forschung und Technologie (HIV-Verbund), and the Max-Planck-Gesellschaft. B.M.W. and T.R. were supported by a stipend from the German Bundesministerium für Bildung, Wissenschaft, Forschung und Technologie (Stipendienprogramm Infektionsforschung). B.M.W. acknowledges support by NATO Collaborative Research Grant CRG 950840. S.F.J.L.G. acknowledges support by NIH Grant GM 52263.

* Corresponding author. Tel.: +49 231 1206 386; Fax: +49 231 1206 229; e-mail: birgit.woehrl@mpi-dortmund.mpg.de.

‡ Max-Planck-Institut für Molekulare Physiologie.

§ Case Western Reserve University School of Medicine.

[1] Abbreviations: HIV, human immunodeficiency virus; EIAV, equine infectious anemia virus; RNase H, ribonuclease H; RT, reverse transcriptase; *E. coli*, *Escherichia coli*; HPLC, high-performance liquid chromatography; p/t, primer/template hybrid; aa, amino acid.

S0006-2960(97)03159-0 CCC: $15.00
Published on Web 08/11/1998

demonstrated that upon deletion of the RNase H domain the enzyme is incapable of processive DNA synthesis (*11*). Taken together, these results imply that the RNase H domain of retroviral RTs contributes to the proper binding of primer/template.

In this context, an interesting question is whether the loss of processive synthesis with EIAV p51/51 is only due to a modification of DNA binding. In addition, deletion of the RNase H domain could lead to a conformational change of the two subunits in the homodimer that in turn leads to alterations in the geometry of the polymerase catalytic site. Since EIAV p51/51 is an active polymerase, this suggests its two identical subunits are present in different conformations, based on knowledge of the 3-D structure of HIV-1 RT. However, since no crystal structure of a homodimeric RT is available, it has not been shown whether the two subunits in the homodimer assume similar conformations as the subunits in the heterodimeric enzyme and whether the structure of the polymerase active site is the same.

In the work reported here, we have analyzed the dimerization and the polymerase activities of the distributive EIAV p51/51 RT in comparison with the processive heterodimeric EIAV p66/51 RT to obtain information about possible conformational differences of their polymerase active sites. We have used pre-steady-state and steady-state kinetic methods to evaluate the nucleic acid binding affinities and the mechanism of nucleotide incorporation of the two enzymes.

EXPERIMENTAL PROCEDURES

Cloning of the EIAV p66/51 Coexpression Vector. For cloning of the p6H-EIAV66/51 coexpression plasmid, the plasmids p6H-EIAVRT66 (*12*) and p6H-EIAVRT51 (*8*) were used. Both plasmids are derivatives of the expression vector pDS56RBSII (*13*) and contain the genes for the EIAV p66 and p51 RT, respectively, with codons for an additional six histidines added to their 5′ ends. An *Xho*I/*Pvu*II expression cassette consisting of the promoter/operator (P/O) region, the coding region for the EIAV p51/51 RT, and the transcriptional terminator was cut out from plasmid p6H-EIAVRT51 and cloned into the *Nde*I site of plasmid p6H-EIAVRT66. Before ligation, the linearized plasmid p6H-EIAVRT66 and the *Xho*I/*Pvu*II fragment were treated with T4 DNA polymerase to obtain blunt-ended fragments. Only plasmids which contained the EIAV RT expression cassettes for p66 and p51 in opposite orientation were recovered. The newly obtained construct p6H-EIAV66/51 is shown in Figure 1. Induction kinetics with the *E. coli* strain M15/pDMI.1 (*13*) transformed with p6H-EIAV66/51 showed higher expression levels of the p51 subunit.

Buffers. RT buffer contained 50 mM Tris-HCl, pH 8.0, 6 mM $MgCl_2$, 0.05% (v/v) Triton X-100, 5 mM NaCl, and 5 mM dithiothreitol. Annealing buffer consisted of 20 mM Tris-HCl, pH 7.5, and 50 mM NaCl. Reaction buffer contained 50 mM Tris-HCl (pH 8.0), 10 mM $MgCl_2$, and 5 mM KCl. HPLC buffer consisted of 50 mM Tris-HCl, pH 8.0, and 150 mM KCl. RT-D buffer contained 50 mM Tris-HCl, pH 7.0, 25 mM NaCl, 1 mM EDTA, 1 mM dithiothreitol, and 10% glycerol. Urea loading buffer contained 7 M urea in Tris/borate/EDTA buffer with 0.1% xylene cyanol and bromphenol blue.

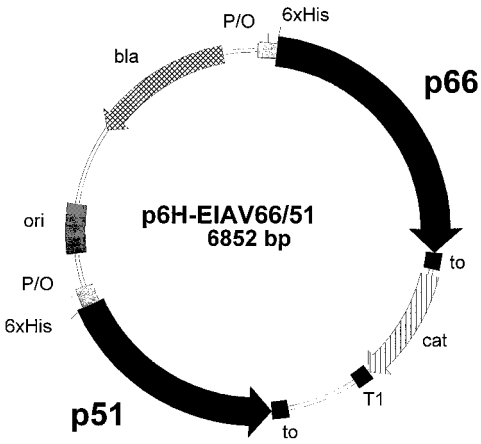

FIGURE 1: Construct for the coexpression of the 66 and 51 kDa subunits of EIAV reverse transcriptase. The coding regions of p51 and p66 and the orientation of the reading frames are indicated by black arrows. ori, origin of replication; to, transcriptional terminator from phage lambda; bla, gene for β-lactamase; cat, gene for chloramphenicol acetyltransferase; T1, transcriptional terminator from the *E. coli rrnB* operon.

Preparation and Purification of EIAV p66/51 and EIAV p51/51. Enzyme purification was similar to that described (*8, 12*); 1 M NaCl was included in the homogenization buffer in order to dissociate nucleoprotein complexes and to inhibit proteases. The high-speed supernatant was loaded on a Ni^{2+}-nitrilotriacetic acid Sepharose (Qiagen) column and eluted with a 0−0.5 M imidazole gradient. RT-containing fractions were pooled, dialyzed against RT-D buffer, and loaded on a DEAE-Sepharose column equilibrated with the same buffer. The flow through of the column was then applied onto a SP Sepharose column (Pharmacia) and eluted with a 0−0.5 M NaCl gradient. Samples were concentrated and dialyzed against HPLC buffer.

To isolate pure EIAV p51/51 homodimer, about 3 mg of the dialyzed protein was further purified by HPLC gel filtration using a Superdex 200 HR10/30 column (Pharmacia). The column was eluted with HPLC buffer at 0.7 mL/min, and the fractions containing homodimer were pooled and concentrated in Microcon 10 tubes (Amicon) and stored in RT-D buffer with 50% glycerol at −20 °C. The dimer content of the concentrated EIAV p51/51 protein amounted to about 80%.

To separate the heterodimeric EIAV p66/51 from remaining excess p51 protein, the RT was further purified by hydrophobic interaction chromatography. After HPLC gel filtration, enzyme was dialyzed against buffer A, containing 10 mM Tris-HCl, pH 7, and 1 M $(NH_4)_2SO_4$, and loaded onto a phenyl-Sepharose (High-Sub) column (Pharmacia). The proteins were eluted by applying a linear gradient of the loading buffer and a buffer (=buffer B) containing 10 mM Tris-HCl, pH 7. The heterodimer eluted at 55% of buffer B, EIAV p51 at 80% of buffer B. The enzyme was concentrated by a vacuum concentrator (Schleicher & Schuell) and stored at −20 °C in RT-D buffer containing 50% glycerol. The purified RTs were free of nuclease contamination.

Oligodeoxynucleotides. Oligodeoxynucleotides were synthesized on an Applied Biosystems 380 B DNA synthesizer and purified by HPLC on a reversed-phase column by standard procedures (*14*) or by denaturing polyacrylamide

gel electrophoresis (15% acrylamide, 7 M urea) followed by elution from the gel using the Schleicher & Schuell Biotrap unit. The sequence of the 18/36mer DNA/DNA primer/template (p/t) was 5′-TCCCTGTTCGGGCGCCAC and 5′-TGTGGAAAATCTCATGCAGTGGCGCCCGAACAGGGA, respectively. The complementary regions are equivalent to the primer binding site sequence from HIV-1. The sequence of the fluorescently labeled FAM primer oligodeoxynucleotide was identical to the one above with the fluorescent label at the 5′ end. The sequence of the mansyl-labeled primer was 5′-TCCCTGTTCGGGCGCC(T-$_{mansyl}$)C. For the mansyl-labeled primer, the following template was used: 5′-TGTGGAAAATCTCATGCAGAGGCGCCCGAACAGGGA. The FAM- and mansyl-labeled oligodeoxynucleotide were synthesized as described previously (*15*, *16*). The mansyl label was introduced at the next to the last nucleotide at the 3′ end of the 18mer primer (*16*). The sequence of the primer used for the DNA/RNA p/t was 5′-TTGTCCGTGTTCGGGCGCCA. The corresponding RNA template was obtained by in vitro transcription (see below) and had the following sequence: 5′-GGGUUAAUCUCUGCAUGGCGCCCGAACAGGGACAA.

Primer oligodeoxynucleotides were 5′ end-labeled with T4 polynucleotide kinase as described (*16*). Primer and template oligodeoxynucleotides were annealed by heating equimolar amounts in annealing buffer for 2 min at 90 °C, followed by cooling to room temperature over 1 h in a water bath. The completeness of the reaction was checked by determining whether 100% of the primer of the hybridized and radioactively labeled p/t could be extended by one nucleotide.

Preparation of RNA. The standard 10 mL T7 RNA polymerase reaction mixture for in vitro transcription contained 40 mM Tris-HCl, pH 8.1, 1 mM spermidine, 0.01% Triton X-100, 50 μg/mL bovine serum albumin (RNase free, Boehringer Mannheim), 8% (w/v) polyethylene glycol 8000, 40 mM dithiothreitol (freshly prepared), 100 mM KCl, 20 mM $MgCl_2$, 4 mM each rNTP (Pharmacia), 1 μM template, and 0.1 mg/mL T7 RNA polymerase. After incubation at 37 °C for 2 h, the reaction was stopped by addition of 50 mM EDTA. The RNA was extracted twice with phenol/chloroform/isoamyl alcohol and precipitated with 1 volume of 2-propanol plus 0.5 M LiCl for 20 min on ice. The pellet then was washed twice with 70% ethanol, dried, and redissolved in 1 mL of water. The sample was mixed 1:1 with formamide loading buffer (*17*) and heated to 80 °C for 2 min, and 1 mL was loaded immediately on a 20% denaturing polyacrylamide gel. The desired band was eluted from the gel, and the RNA was precipitated as described above and finally stored at − 80 °C.

Polymerase Activity Determination. RNA-dependent DNA polymerase activity on poly(rA)/oligo(dT)$_{12-18}$ substrates was measured by a standard assay (30 μL reaction volume) described previously (*18*) with 5−10 ng of enzyme in RT buffer. Under these conditions, 1 unit of RT activity catalyzes the incorporation of 1 nmol of dTTP into poly(rA)/oligo(dT)$_{12-18}$ in 10 min.

Fluorescence Equilibrium Titrations with Primer/Template. Fluorescence titrations were performed using an SLM Smart 8100 spectrofluorometer equipped with a PH-PC 9635 photomultiplier. Extrinsic fluorescence measurements with the FAM-labeled p/t substrate were performed in reaction buffer in a total volume of 1 mL as described previously. The excitation wavelength was at 492 nm, and the emission intensity was measured at 516 nm (slit width set at 1 and 8 nm for excitation and emission, respectively) (*19*). Values for the dissociation constant (K_d) were determined as described previously using the data fitting program 'Grafit' (Erithacus Software) (*14*). A quadratic equation analogous to the one given by (*14*) was used for the fitting procedure.

Affinities for the DNA/RNA p/t substrate were determined by displacing a fluorescently labeled 18/36mer DNA/DNA p/t complexed with RT. A 25 nM aliquot of the FAM-labeled DNA/DNA p/t was preincubated with 50 nM EIAV p66/51 or 100 nM EIAV p51/51. The DNA/DNA substrate was then displaced by titration with the DNA/RNA p/t. The fluorescence changes upon displacement were monitored as described above and evaluated as described using the program "Scientist" (*16*).

Rapid Kinetics of Primer/Template Binding. Experiments on the kinetics of the association of EIAV RT with a labeled p/t were performed in reaction buffer using a stopped-flow apparatus (High Tech Scientific, Salisbury, England). A 50 nM sample of a mansyl-labeled 18/36mer p/t DNA (final concentration) was rapidly mixed with increasing RT concentrations (150−500 nM). Collection and analysis of the data were done as described previously (*16*). The two phases were fitted using a double-exponential equation. The rate of the first phase is dependent on the concentration of RT (*20*). The linear fit of the concentration dependence yields k_{+1} and k_{-1} of p/t binding. The rate k_{+2} of the second phase is largely concentration-independent at the concentrations used and describes the conformational change of RT−p/t binding.

Rapid Kinetics of Nucleotide Incorporation. Rapid quench experiments were carried out in reaction buffer in a rapid quench apparatus built by KinTek Instruments (University Park, PA) as described previously (*15*, *16*). Quantification of the data was achieved by phosphorimaging. All concentrations reported are final concentrations after mixing in the rapid quench apparatus. Data were fitted to a burst equation (double-exponential plus slope) using the program 'Grafit'. The pre-steady-state rates k_{pol1} and k_{pol2} are given by the exponentials (*21*). The burst amplitude is composed of the sum of the two exponential phases and corresponds to the amount of RT bound to p/t at the beginning of the reaction ($t = 0$). When p/t is in excess to RT, the slope of the curve corresponds to the dissociation of RT from p/t during the steady-state phase. k_{diss} is calculated by the slope divided by the burst amplitude (*21*).

RESULTS

Enzyme Preparation and Dimer Stability. After purification of the EIAV p66/51 heterodimer and the p51 homodimer, the dimer content of the two enzymes was determined by HPLC size-exclusion chromatography (Figure 2b). EIAV p51/51 RT is contaminated with about 20% of the monomeric protein. However, as with HIV-1 RT, the monomeric subunits did not show activity (*6*). In contrast to the situation with HIV-1 RT, it was not possible to achieve dimerization of the remaining monomeric protein upon concentration of the protein solution (data not shown). We assume that due to overexpression of the p51 subunit, a portion of the protein cannot be folded correctly during

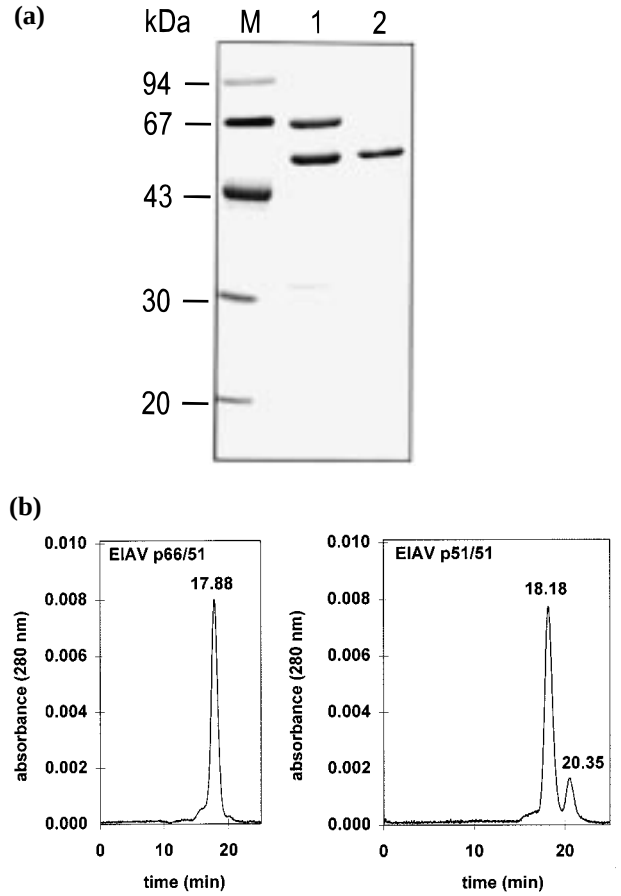

FIGURE 2: Analysis of the purified EIAV p66/51 and EIAV p51/51 RTs by SDS−polyacrylamide gel electrophoresis and HPLC size-exclusion chromatography. (a) SDS−polyacrylamide gel electrophoresis. Proteins were detected by silver staining (BioRad kit). Lane M, protein molecular mass markers in kDa. Lane 1, EIAV p66/51 RT; lane 2, EIAV p51/51 RT. (b) HPLC size-exclusion chromatography of purified RTs. Six micrograms of purified EIAV p66/51 and EIAV p51/51 RTs was analyzed at room temperature. The retention times were 17.88 min for the heterodimer, 18.18 min for the homodimeric p51, and 20.35 min for the monomeric p51. The molecular masses were determined using molecular mass standard proteins from BioRad.

bacterial growth. Since the monomeric protein also contains the N-terminal His-tag, it is copurified together with the homodimer. During the last purification step of EIAV p51/51, i.e., preparative HPLC gel filtration, the dimer and the monomeric proteins can be separated. For the last step in the purification of EIAV p66/51 RT, we used hydrophobic interaction chromatography to eliminate excess p51 monomer. Figure 2b shows that the purified EIAV p66/51 RT is free of excess p51 and completely dimeric. The purity of both enzymes is indicated in Figure 2a.

In a preliminary assay, the RNA-dependent DNA polymerase activities of the purified enzymes were determined on the homopolymeric substrate poly(rA)/oligo(dT)$_{12-18}$. The specific activity of the p66/51 heterodimer was about 3.5-fold higher (247 units/μg of protein) than that of the p51 homodimer (71 units/μg of protein).

For heterodimeric HIV-1 RT, it has been demonstrated that it can be fully dissociated by adding 15% acetonitrile to the protein solution and reassociated by diluting the solution 4-fold (*6*, *22*). The fact that EIAV p51/51 RT is a more stable dimer than its HIV-1 p51 counterpart indicates

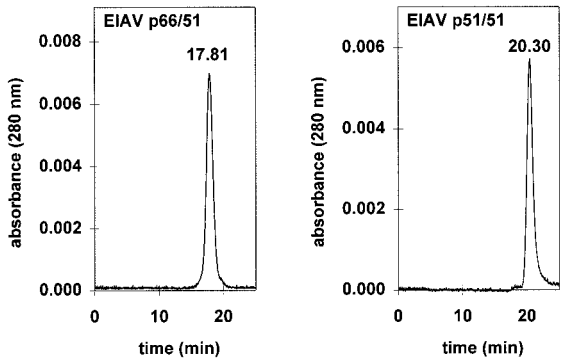

FIGURE 3: HPLC size-exclusion chromatography of EIAV p66/51 and EIAV p51/51 RTs after treatment with 15% acetonitrile. Six micrograms of EIAV p66/51 or EIAV p51/51 RT was analyzed after treatment of the RT solutions with 15% acetonitrile. EIAV p66/51 remains completely dimeric whereas the subunits of EIAV p51/51 RT can be separated and only the monomer is detected.

stronger interactions of the two subunits. To analyze the dimer stability, we added increasing amounts of acetonitrile (5−20%) to solutions of the two EIAV RT variants. The dimer content of the proteins was analyzed after an incubation time of 15 min at room temperature. Our results show that p51 EIAV RT dissociates completely after the addition of 15% acetonitrile (Figure 3). However, in contrast to the results obtained with HIV-1 RT, no reassociation into dimeric protein was observed after a 4-fold dilution of the solution. To exclude an effect of the dilution on dimerization, the enzyme was concentrated in Microcon tubes (Amicon). This method helps to avoid reconcentration of acetonitrile during concentration of the protein. However, even after incubation of the concentrated enzyme solution for 8 h on ice or at room temperature, no reassociation was observed, indicating an irreversible conformational change upon monomerization.

With EIAV p66/51, no dissociation of the dimer could be obtained at 15% acetonitrile (Figure 3), and higher acetonitrile concentrations led to precipitation of the protein. We therefore assume that probably stronger hydrophobic interactions between the two subunits are responsible for the dimer stability. However, we cannot exclude the possibility that a greater contribution from hydrophilic interactions than in HIV-1 RT plays a stabilizing role.

Primer/Template Binding. DNase I protection analyses of replication complexes containing homodimeric EIAV p51/51 or EIAV p66/66 RT already indicated that the absence of the RNase H domain in EIAV p51/51 reduces the stability of the RT/DNA complex. Partial DNase I treatment of the EIAV p51/51/DNA complex did not lead to a footprint, whereas with the EIAV p66/66 enzyme a footprint could be obtained (*9*).

Fluorescence equilibrium titrations were performed to determine the affinity of EIAV p66/51 and EIAV p51/51 RT to a fluorescently labeled 18/36mer DNA/DNA substrate. We have shown previously with HIV-1 RT that the fluorescent FAM label at the 5′end of the primer does not significantly influence the affinity of RT for its nucleic acid substrate and can therefore be used as a signal to measure binding (*15*). Figure 4 shows the titration curves obtained with EIAV p66/51 and EIAV p51/51 RT. The different degrees of fluorescence quenching obtained are probably due to a different environment of the FAM label in the two enzymes. Since the label is at the 5′ end of the primer, it is

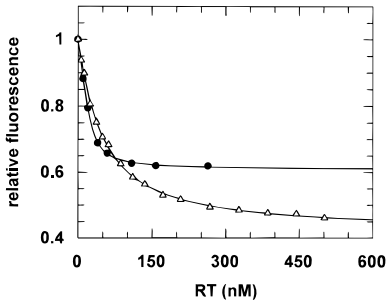

FIGURE 4: Fluorescence equilibrium titrations with p/t DNA. A 20 nM aliquot of FAM-labeled p/t DNA was titrated with EIAV p66/51 (●) or EIAV p51/51 (△) at 25 °C in reaction buffer using the decrease of the fluorescence as a signal for binding. The curves show the best fit to a quadratic equation describing the binding equilibrium with K_d values of 4 and 40 nM for p66/51 and p51/51, respectively (see also Table 1).

located in the vicinity of the RNase H domain in the heterodimer. However, this domain is missing in the homodimer. Analysis of the data reveals a K_d value for the homodimeric EIAV p51/51 enzyme that is 10-fold higher than that of the wt EIAV p66/51 RT (Table 1). This result suggests that the distributive mode of polymerization observed with EIAV p51/51 RT (*8*) on DNA substrates is at least in part due to the reduced affinity for DNA.

In addition, the affinities for an 20/35mer DNA/RNA p/t were determined by displacing the fluorescently labeled DNA/DNA p/t in the RT−p/t complex with the unlabeled DNA/RNA p/t (data not shown). Evaluation of the data led to K_d values for EIAV p66/51 and EIAV p51/51 of <0.5 nM and of about 14 nM, respectively, indicating a tighter binding of DNA/RNA substrates of both enzymes.

For HIV-1 RT, it has been shown that the binding of p/t DNA takes place in several steps. First a concentration-dependent step is observed that leads to the formation of a collision complex, which is then succeeded by a conformational change to form a tight RT−p/t complex with an overall K_d in the nanomolar range (*20, 23*). To analyze which step of p/t binding is impaired with EIAV p51/51 RT, we used pre-steady-state kinetic techniques. Stopped-flow measurements were performed with a DNA/DNA p/t to obtain the rate constants for the first and the second step of p/t binding.

For rapid mixing studies in the stopped-flow instrument, a p/t was used with a mansyl group attached at the next to the last nucleotide of the 3′ end of the primer. Figure 5 shows a typical stopped-flow result obtained with EIAV p66/51 RT under pseudo-first-order conditions. Similar to HIV-1 RT, EIAV p66/51 and EIAV p51/51 appear to bind p/t in two phases: a rapid first phase leading to a fluorescence increase which reflects the relatively weak initial binding and a second slow phase leading to a decrease of the fluorescence signal, which represents the conformational change yielding k_{+2} in the scheme of Rittinger et al. (*20*). In Figure 6 the concentration dependence of the pseudo-first-order rate constant of p/t binding is shown with both enzymes. The slope of the line yields the association rate constant k_{+1}, and the intercept with the *y*-axis yields the dissociation rate constant k_{-1}. The values for k_{+1} and for the isomerization step k_{+2} were essentially the same for the two enzymes (Table 1). However, k_{-1} obtained with EIAV p51/51 is about 17.4-fold higher than that of the EIAV p66/51 enzyme. These data show that the reduced affinity for p/t of EIAV p51/51 RT is correlated at least partially to a faster dissociation of the p/t from the enzyme from the first bound state. However, as described below, the dissociation rate constant for the second step k_{diss} is also different for the two enzymes.

Kinetics of Nucleotide Incorporation. In addition to the increased dissociation rate for p/t from the first bound state, deletion of the RNase H domain could lead to conformational changes in the p51 homodimer or of the enzyme−p/t complex that influence the kinetics of nucleotide incorporation with EIAV p51/51. To address this question, we used the quench flow method (*21*) to measure the pre-steady-state rate constant of the incorporation of a single nucleotide into a radiolabeled 18/36mer DNA/DNA p/t and a 20/35mer DNA/RNA p/t substrate. Figure 7a shows the typical time dependence of dTTP incorporation with a complex of 100 nM EIAV p66/51 and 200 nM DNA/DNA p/t at a concentration of 100 μM dTTP.

Under the conditions used for EIAV p66/51 (Figure 7a), EIAV p51/51 yields a small overall burst amplitude (Figure 7b) since due to its low affinity for DNA/DNA p/t the RT concentration is not saturating. To test whether the dTTP concentration was saturating, nucleotide incorporation with EIAV p51/51 was assayed at elevated dTTP concentrations of 1 and 2.5 mM. However, no increase of the burst rate was observed (data not shown). To determine the two phases of the burst more precisely, a higher enzyme concentration of 500 nM was used for EIAV p51/51 (Figure 7b). The best fit for both enzymes was obtained by fitting the data to a burst equation with two exponentials plus slope. When p/t is in excess to RT, the slope reflects the slow steady-state phase and yields k_{diss}. The two exponential phases reflect the amount of RT that is bound to p/t in a productive manner at the beginning of the reaction. The burst obtained with HIV-1 RT on DNA/DNA substrates has previously been described by only one exponential phase (*21*). However, a more precise analysis of the data obtained with HIV-1 RT on DNA substrates shows that the burst is also composed of two exponential phases, similar to those found here with EIAV RT (B.M.W. and R.K., unpublished results). For comparison, the fits obtained by a burst equation with one exponential are shown by dotted line for the two enzymes.

Comparison of the maximal pre-steady-state burst rates for nucleotide incorporation (k_{pol1} and k_{pol2}) indicates that the low affinity of EIAV p51/51 for DNA/DNA p/t does not have a large effect on the achievable incorporation rates. A fraction of the EIAV p51/51−p/t complex incorporates dTTP with almost the same high rates as the EIAV p66/51 enzyme. However, the amplitudes of the two burst phases differ significantly for the two enzymes (Table 2). With EIAV p51/51, the faster first exponential phase represents only ca. 13% of the total burst amplitude, whereas with EIAV p66/51 the first phase is about 43% of the total amplitude. These data imply that loss of the RNase H domain results in a different nucleotide incorporation behavior of EIAV p51/51. Additionally, the steady-state rate (k_{diss}) of EIAV p51/51 is 7-fold increased due to the faster rate-limiting product dissociation step (Table 2).

The results obtained with a DNA/RNA p/t are different (Figure 7c). Obviously, the burst amplitudes are much larger, which could in part be due to the higher affinity of both enzymes for this substrate. This observation is especially

Table 1: Parameters for p/t (DNA/DNA) Binding

enzyme	K_d (nM)	k_{+1}(x10^9 M^{-1} s^{-1})	k_{-1} (s^{-1})	k_{+2} (s^{-1})
EIAV p66/51	4 (±0.6) (DNA/RNA: <0.5)	1.31 (±0.02)	8.9 (±7.37)	12 (±1.5)
EIAV p51/51	40 (±1.2) (DNA/RNA: 14)	0.78 (±0.013)	155 (±3.75)	12 (±0.4)

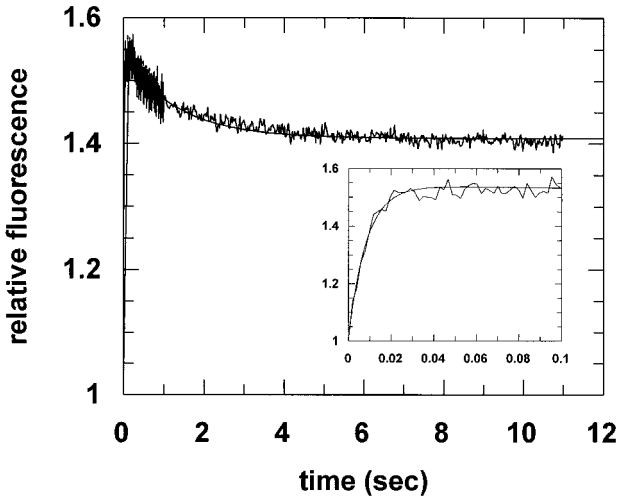

FIGURE 5: Kinetics of binding of a fluorescently labeled p/t DNA to EIAV p66/51 RT. A typical stopped-flow result obtained is shown. A 50 nM sample of p/t was rapidly mixed with 200 nM RT. Excitation was at 364 nm, and emission was detected via a cutoff filter (389 nm).

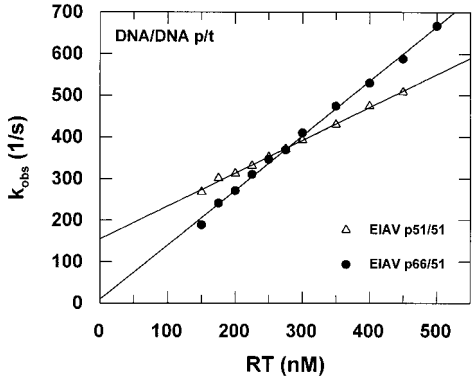

FIGURE 6: Dependence of the pseudo-first-order rate constant of p/t binding on the RT concentration. A constant concentration of the fluorescently labeled p/t of 50 nM and increasing concentrations of EIAV p66/51 (●) or EIAV p51/51 (△) were used to determine the observed rate constants for each concentration. The slope of the linear fit yields k_{+1}; the intercept with the *y*-axis yields k_{-1}. The values for k_{+1} and k_{-1} with EIAV p66/51 are 1.31×10^9 M^{-1} s^{-1} and 8.9 s^{-1}, respectively. With EIAV p51/51, k_{+1} is 0.78×10^9 M^{-1} s^{-1} and k_{-1} equals 155 s^{-1}. For k_{+2}, values of 12 s^{-1} were obtained for both enzymes. A summary is shown in Table 1.

striking with the homodimeric EIAV p51/51 where the total burst amplitude using 100 nM RT reaches about 89 nM as compared to about 15.9 nM using the DNA/DNA substrate. Also, contrary to the results obtained with the DNA/DNA p/t, almost all of EIAV p66/51 is bound to the substrate at the beginning of the reaction, yielding a total burst amplitude of 93 nM. In addition, the maximal burst rates obtained for the two enzymes are comparable. Due to the very high affinity of EIAV p66/51 for the DNA/RNA p/t (K_d < 0.5 nM), the value for k_{diss} is much lower (0.007 s^{-1}) than the value obtained with EIAV p51/51 ($k_{diss} = 0.1$ s^{-1}). Our data indicate that the binding of the RTs to DNA/RNA p/t is different from the binding to DNA/DNA substrates.

DISCUSSION

We have shown previously that the heterodimeric EIAV p66/51 and the homodimeric EIAV p66/66, similar to their HIV-1 counterparts, polymerize DNA in a processive mode whereas EIAV p51/51 and HIV p51/51 show a distributive mode of polymerization (*8*, *9*). Experiments presented in this paper help to understand the different modes of polymerization found between homo- and heterodimeric RT enzymes of closely related retroviruses such as EIAV, HIV-1, and HIV-2. In addition, these analyses provide valuable information on the structure of homodimeric RT.

EIAV RT was chosen to compare the mechanism of polymerization of the p66/51 and p51/51 variants because in contrast to its HIV-1 counterparts stable dimeric proteins are formed (*8*). This result was confirmed by the data presented here (Figure 3). Under conditions where monomerization of the stable heterodimeric HIV-1 p66/51 can be observed by the addition of acetonitrile (*6*, *22*), only EIAV p51/51 could be monomerized, but not EIAV p66/51. This result indicates stronger or different interactions between the EIAV RT subunits than between the subunits of HIV-1 RT. Ionic interactions are unlikely to play a decisive role since the purification procedure in a buffer containing 1 M NaCl should then have led to a weakening of such interactions, thus leading to monomeric protein.

Comparative analysis of the dimer stability of HIV-1 and HIV-2 RT showed that the latter also forms a more stable dimer (*24*, *25*). Differences in secondary structure could be responsible for this result. Secondary structure predictions with HIV-2 RT using the protein structure prediction program SOPM (*24*) reveal a possible structural variance between HIV-1 and HIV-2 RT in a region located in the junction between the thumb and connection subdomains between amino acids 312 and 332. In this area, the crystal structure of HIV-1 RT shows the formation of two β-strands whereas for HIV-2 RT an α-helix is predicted. Computer analysis of EIAV RT with the program 'PredictProtein' (http://www.embl.heidelberg.de/predictprotein/) also predicts an α-helix in this area. Amino acid comparison of this region between the three RTs shows that both EIAV RT and HIV-2 RT, but not HIV-1 RT, contain a stretch of glutamic acid residues that is probably responsible for the formation of an α-helix. The motif QEEEELE is found at positions 320−326 in the HIV-2$_{D194}$ isolate while the region at positions 323−330 in EIAV RT possesses the sequence PEEEMLCE. In addition to this region, a tryptophan motif, TWETWWTEYWQ, between amino acids 396 and 406 in HIV-1 RT appears to be important for dimerization (*24*, *26*). Again, this region looks different in EIAV RT and lacks two of the four tryptophan residues (aa 399−408: MWEMQKGWYY). We assume that these alterations in the EIAV RT sequence

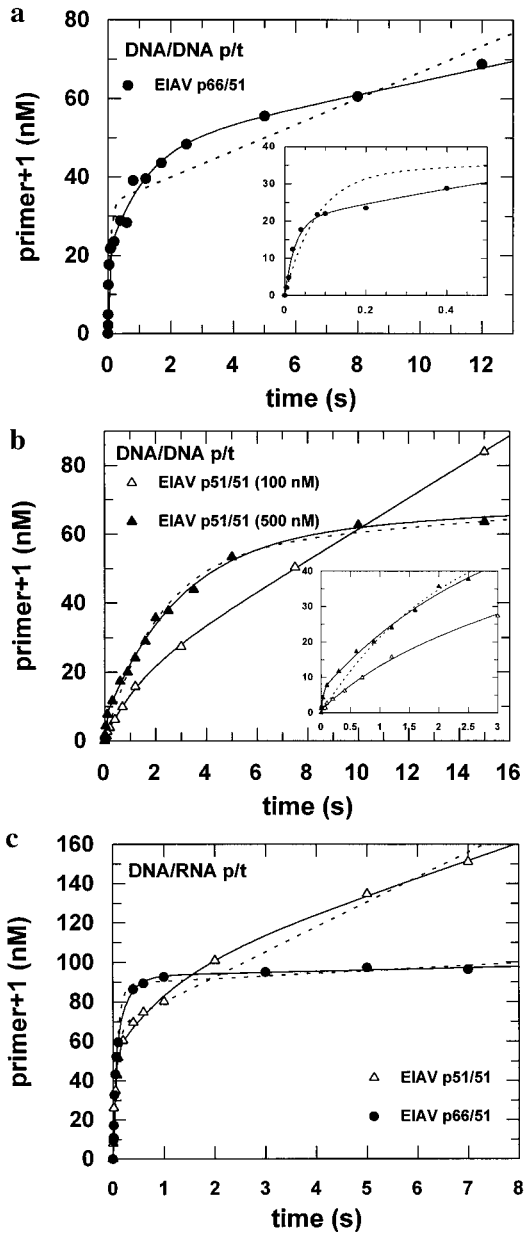

FIGURE 7: Kinetics of nucleotide incorporation with EIAV p66/51 and EIAV p51/51 RT. Data were fitted to a double-exponential equation plus slope. The best fits obtained with a single-exponential equation plus slope are shown by dotted lines. (a) A preformed complex of 200 nM DNA/DNA p/t and 100 nM EIAV p66/51 was mixed with 100 μM dTTP. The maximal values obtained for the burst rates k_{pol1} and k_{pol2} are 40 s^{-1} and 0.9 s^{-1}, respectively. The reduced χ^2 value obtained equals 3.38 for the double-exponential and 22.9 for the single-exponential fit. (b) A preformed complex of either 200 nM DNA/DNA p/t and 100 nM EIAV p51/51 (△) or 100 nM p/t DNA/DNA and 500 nM EIAV p51/51 (▲) was mixed with 100 μM dTTP. (The reduced χ^2 for the double-exponential fit at 500 nM RT equals 1; for the single-exponential fit, the reduced χ^2 equals 6.4.) The maximal values for the burst rates k_{pol1} and k_{pol2} are 31.6 s^{-1} and 0.34 s^{-1}, respectively, at an RT concentration of 500 nM. The slope of the curve obtained with 100 nM RT was used to determine k_{diss}. (c) A preformed complex of 200 nM DNA/RNA p/t and 100 nM EIAV p51/51 (△) or 100 nM EIAV p66/51 (●) was mixed with 100 μM dTTP. The maximal values for the burst rates k_{pol1} and k_{pol2} are 22.7 s^{-1} and 0.9 s^{-1}, respectively, for EIAV p51/51 (reduced $\chi^2 = 11$ for the double-exponential and 25.6 for the single-exponential fit) and 24.1 s^{-1} and 4.3 s^{-1}, respectively, for EIAV p66/51 (reduced $\chi^2 = 2.5$ for the double-exponential and 8.2 for the single-exponential fit). A summary of the data is shown in Table 2.

contribute to a change in the geometry of the dimer, leading to a more 'closed conformation' of the enzyme that stabilizes the dimer state. Therefore, the enzyme is less sensitive to the organic solvent acetonitrile.

Analysis of the kinetics of p/t binding suggests that the distributive phenotype of polymerization associated with the homodimeric EIAV enzyme is at least in part due to a decrease in the affinity for p/t substrates. Both k_{-1} (the rate constant for dissociation from the first bound state) and k_{diss}, as estimated from the rate of the steady-state phase, are increased in EIAV p51/51 RT. The decrease in affinity for p/t makes it more likely for EIAV p51/51 as compared to the p66/51 heterodimer to dissociate from p/t before a long stretch of nucleotides can be incorporated. The kinetic parameters given in Table 1 can be used to calculate the expected K_d values. If this is done, values are obtained which are smaller than those measured directly. There are several possible factors contributing to this discrepancy. One is that some values obtained are for fluorescently labeled p/t, while values from quenched-flow experiments are for unlabeled p/t. There are two main sources of error in determining the K_d values for EIAV p66/51 and EIAV p51/51. For EIAV p51/51, the dissociation rate obtained from the steady-state phase of the incorporation kinetics is poorly determined due to the small burst amplitudes and difficulty of distinguishing the phases (Figure 7b). Thus, it is quite possible that k_{diss} is considerably higher than the value obtained, increasing the calculated K_d. For EIAV p66/51, the value of the *y*-axis intercept that yields k_{-1} could be higher (Figure 6), which will also increase the calculated K_d value. Thus, the discrepancy between the measured and calculated K_d values cannot be taken as an indication that an error has been made in assigning the mechanism or constants for p/t binding based on the present results.

Only minor alterations in the maximal burst rates for nucleotide incorporation were obtained with EIAV p51/51 as compared to the heterodimeric RT. Two pre-steady-state phases were observed with both enzymes for the DNA/DNA as well as the DNA/RNA substrate. However, with the DNA/DNA p/t, the relative amplitude of the faster first phase is significantly lower for EIAV p51/51 than for EIAV p66/51 RT whereas the amplitude of the second slower phase is larger (Table 2). We cannot yet provide a definitive explanation of the biphasic nucleotide incorporation kinetics. Here, we suggest a model in which the two burst phases could represent a slow conformational change of the p/t substrate from an unfavorable nonproductive form into a more favorable and thus more active conformation. In this model, the first fast phase would represent an RT−p/t complex in the favorable productive conformation for nucleotide incorporation, whereas the slower second burst phase would represent an RT−p/t complex in the less favorable conformation that has to undergo a conformational change in order to be able to incorporate nucleotide. Alternatively, the second phase could represent an unfavorable complex which is not in equilibrium with the other complex but is able to incorporate nucleotide at a reduced rate. We are not able to distinguish between these possibilities with the available data. Whichever alternative is correct, we conclude that with DNA/DNA substrates a significantly smaller fraction of the enzyme−substrate complex is in the active or more active conformation with EIAV p51/51 than

Table 2: Parameters for Incorporation of dTTP into DNA/DNA and DNA/RNA p/t

primer/template	enzyme	k_{pol1} (s^{-1})	amplitude 1 (nM)	k_{pol2} (s^{-1})	amplitude 2 (nM)	k_{diss} (s^{-1})
DNA/DNA	EIAV p66/51	40 (±10)	19.7 (±2)	0.9 (±0.5)	26.5 (±12)	0.04
	EIAV p51/51	31.6 (±13.3)[a]	6.1 (±0.8)[a]	0.34 (±0.02)[a]	54.1 (±1.9)[a]	0.28
DNA/RNA	EIAV p66/51	24.1 (±4.9)	49.9 (±9.7)	4.3 (±1.14)	43.1 (±9)	0.007
	EIAV p51/51	22.7 (±4.8)	52.5 (±5.2)	0.9 (±0.65)	37 (±11.5)	0.1

[a] Values obtained at 500 nM EIAVp51/51.

with EIAV p66/51. However, our results with the DNA/RNA p/t demonstrate very clearly that EIAV p51/51 is able to incorporate nucleotides as effectively as the heterodimer and with similar burst amplitudes. In this case, the major difference between the two enzymes is not the burst rate or amplitude but the difference in k_{diss} (Figure 7c). These results imply that the total burst amplitude of only 42% obtained for EIAV p66/51 with the DNA/DNA p/t is not due to a portion of inactive enzyme in our preparation since we obtain the theoretically expected burst amplitudes with the DNA/RNA p/t. We are presently investigating the reasons for the different nucleotide incorporation behavior obtained with different nucleic acid substrates (manuscript in preparation).

Our data show that EIAV p51/51 behaves similarly to the heterodimeric enzyme using a DNA/RNA substrate (Figure 7c and Table 2). This may be connected with the fact that in general, DNA/DNA duplexes assume the B-conformation whereas DNA/RNA duplexes adopt an A-like conformation. The crystal structure of HIV-1 RT complexed with an 18/19mer p/t DNA/DNA substrate shows that in the region close to the polymerase active site the DNA assumes an A-like form. At the RNase H catalytic center, the DNA is bound in its normal B-form. Between the two stretches, the DNA is bent by 40−45° (*27*). It is assumed that this peculiar DNA conformation is induced upon binding of RT to the p/t DNA. This model is supported by the crystal structure of T7 DNA polymerase and *Bacillus* DNA polymerase (*28*, *29*). The latter could be resolved recently with a catalytically active crystal. The polymerase complexed to DNA shows extensive sequence-independent interactions in the minor groove of the first four base pairs extending from the 3′ terminus of the primer. These interactions are only possible by significant underwinding of the DNA. This leads to a switch of the sugar pucker of the C2′ endo conformation characteristic for B-form DNA to the C3′ endo conformation characteristic for A-form DNA. In addition, the minor groove is widened and becomes more shallow [for review, see (*30*, *31*)].

Probably the conformational changes that have to be imposed on a DNA/RNA p/t are not that drastic since the substrate is already in an A-like conformation. We believe that the reason for the higher burst amplitude we obtain with the DNA/RNA p/t as compared to the DNA/DNA p/t is possibly due to the conformational differences between the two substrates. Experiments to prove this hypothesis are currently performed.

Our results show that a small fraction of the EIAV p51/51−DNA/DNA complex and a significantly larger fraction of the EIAV p51/51−DNA/RNA complex are able to incorporate nucleotide with similar rates as EIAV p66/51 (Table 2), implying that the polymerase active site of the EIAV p51/51 homodimer can exist in a form more or less identical to that of the heterodimeric p66/51 enzyme. However, since more enzyme is in the unfavorable conformation for nucleotide incorporation with DNA/DNA p/t and in addition the k_{diss} values for EIAV p51/51 are increased for both substrates, the whole polymerization process is slowed. Together with the reduced p/t binding activity this leads to the lower specific activity observed for EIAV p51/51 and probably contributes to its distributive mode of polymerization, since it is the ratio of the effective rate of polymerization to the dissociation rate (k_{pol}/k_{diss}) which determines processivity.

A consequence of the results reported here is that the two identical subunits in the homodimeric enzyme can assume conformations similar to the p66 and p51 subunits of the heterodimer in order to perform nucleotide incorporation at similar rates. The crystal structure of the heterodimeric HIV-1 RT shows that interactions between the p66 and p51 subunits are highly asymmetric. The subunit interface on p51 involves different amino acid residues than that of p66. The most important difference in the structures of the two subunits in the heterodimer is the position of the fingers and palm subdomains relative to that of the connection subdomain. In p51, the connection subdomain contacts the fingers and palm subdomains, whereas in p66 the connection subdomain makes no contact with the fingers and almost none with the palm. Relative to its position in p66, the thumb is moved away from the palm and contacts the RNase H domain. As a consequence, the connection domain is folded up between the fingers and the thumb. Thus, in p51 no binding cleft can be formed. In p66, the different folding contributes to the formation of the polymerase active site and a cleft that allows binding of nucleic acid (*27*, *32*, *33*).

From our results, it is apparent that one subunit in EIAV p51/51 can assume a conformation equivalent to that of a p66 subunit in the heterodimer and is thus able to form a polymerase active site, whereas the other subunit looks like the p51 in the p66/51 enzyme. However, since EIAV p51/51 lacks the RNase H domain, it is not able to bind p/t substrates as tightly as EIAV p66/51. In addition, the catalytically competent form of the RT−p/t complex is less stable with EIAV p51/51. Apparently the deletion of the RNase H domain leads to a weakening of the dimer stability and the interaction with p/t that in turn impair the enzyme's ability to form the proper conformation for nucleotide incorporation.

Our conclusions are supported by a recent report (*34*) in which the authors show that the HIV p51/51 is inhibited by an inhibitor of the nonnucleoside class. This group of inhibitors binds to a hydrophobic pocket located close to the polymerase active site in the heterodimeric enzyme. Only one binding site is found in p66/51, and the hydrophobic pocket is not present in p51. Therefore, the authors suggest that the homodimeric enzyme must adopt a conformation similar to p66/51.

It is a quite unusual situation in known protein structures that the subunits of a protein homodimer possess different conformations. X-ray crystallographic data of the HIV-1 protease and the catalytic domain of the integrase, which are both homodimeric enzymes, show a symmetrical conformation of both subunits (*35*, *36*). We therefore suggest that EIAV p51/51 is an interesting candidate for crystallization and structure determination in order to clarify the origins of structural differences in the subunits of a homodimer. However, the results presented suggest that crystallization of complexes between RTs and p/t molecules will generally be complicated by the presence of different forms of the complex which are in equilibrium with each other. This may be the reason it has only been possible so far to solve the HIV-1 RT substrate complex with a p/t of atypical structure (only one 5′ overhanging nucleotide of the template) and an antibody fragment.

ACKNOWLEDGMENT

We thank Karin Vogel-Bachmayr and Martina Wischnewski for excellent technical assistance and Dr. Jason Rausch for helpful discussions.

REFERENCES

1. Lightfoote, M., Coligan, J., Folks, T., Fauci, A. S., Martin, M. A., and Venkatesan, S. (1986) *J. Virol. 60*, 771−775.
2. Di Marzo Veronese, F., Copeland, T. D., DeVico, A. L., Rahman, R., Oroszlan, S., Gallo, R. C., and Sarngadharan, M. G. (1986) *Science 231*, 1289−1291.
3. Kraus, G., Behr, E., Baier, M., Konig, H., and Kurth, R. (1990) *Eur. J. Biochem. 192*, 207−213.
4. Elder, J. H., Schnölzer, M., Hasselkus Light, C. S., Henson, M., Lerner, D. A., Phillips, T. R., Wagaman, P. C., and Kent, S. B. (1993) *J. Virol. 67*, 1869−1876.
5. DeVico, A., Montelaro, R. C., Gallo, R. C., and Sarngadharan, M. G. (1991) *Virology 185*, 387−394.
6. Restle, T., Müller, B., and Goody, R. S. (1990) *J. Biol. Chem. 265*, 8986−8988.
7. Restle, T., Müller, B., and Goody, R. S. (1992) *FEBS Lett. 300*, 97−100.
8. Wöhrl, B. M., Howard, K. J., Jacques, P. S., and Le Grice, S. F. J. (1994) *J. Biol. Chem. 269*, 8541−8548.
9. Rausch, J. W., Arts, E. J., Wöhrl, B. M., and Le Grice, S. F. J. (1996) *J. Mol. Biol. 257*, 500−511.
10. Rausch, J. W., and Le Grice, S. F. J. (1997) *J. Biol. Chem. 272*, 8602−8610.
11. Telesnitsky, A., and Goff, S. P. (1993) *Proc. Natl. Acad. Sci. U.S.A. 90*, 1276−1280.
12. Le Grice, S. F. J., Panin, M., Kalayjian, R. C., Richter, N. J., Keith, G., Darlix, J. L., and Payne, S. L. (1991) *J. Virol. 65*, 7004−7007.
13. Certa, U., Bannwarth, W., Stüber, D., Gentz, R., Lanzer, M., Le Grice, S., Guillot, F., Wendler, I., Hunsmann, G., Bujard, H., and Mous, J. (1986) *EMBO J. 5*, 3051−3056.
14. Müller, B., Restle, T., Reinstein, J., and Goody, R. S. (1991) *Biochemistry 30*, 3709−3715.
15. Wöhrl, B. M., Krebs, R., Thrall, S. H., Le Grice, S. F. J., Scheidig, A. J., and Goody, R. S. (1997) *J. Biol. Chem. 272*, 17581−17587.
16. Krebs, R., Immendörfer, U., Thrall, S., Wöhrl, B. M., and Goody, R. S. (1997) *Biochemistry 36*, 10292−10300.
17. Sambrook, J., Fritsch, E. F., and Maniatis, T. (1994) *Molecular Cloning—A Laboratory Manual*, Cold Spring Harbor Laboratory Press, Cold Spring Harbor, NY.
18. Jacques, P. S., Wöhrl, B. M., Ottmann, M., Darlix, J.-L., and Le Grice, S. F. J. (1994) *J. Biol. Chem. 269*, 26472−26478.
19. Thrall, S. H., Reinstein, J., Wöhrl, B. M., and Goody, R. S. (1996) *Biochemistry 35*, 4609−4618.
20. Rittinger, K., Divita, G., and Goody, R. S. (1995) *Proc. Natl. Acad. Sci. U.S.A. 92*, 8046−8049.
21. Kati, W. M., Johnson, K. A., Jerva, L. F., and Anderson, K. S. (1992) *J. Biol. Chem. 267*, 25988−25997.
22. Divita, G., Restle, T., and Goody, R. S. (1993) *FEBS Lett. 324*, 153−158.
23. Divita, G., Müller, B., Immendörfer, U., Gautel, M., Rittinger, K., Restle, T., and Goody, R. S. (1993) *Biochemistry 32*, 7966−7971.
24. Divita, G., Rittinger, K., Geourjon, C., Deléage, G., and Goody, R. S. (1995) *J. Mol. Biol. 245*, 508−521.
25. Divita, G., Rittinger, K., Restle, T., Immendörfer, U., and Goody, R. S. (1995) *Biochemistry 34*, 16337−16346.
26. Divita, G., Restle, T., Goody, R. S., Chermann, J. C., and Baillon, J. G. (1994) *J. Biol. Chem. 269*, 13080−13083.
27. Jacobo-Molina, A., Ding, J., Nanni, R. G., Clark, A. D., Jr., Lu, X., Tantillo, C., Williams, R. L., Kamer, G., Ferris, A. L., Clark, P., Hizi, A., Hughes, S. H., and Arnold, E. (1993) *Proc. Natl. Acad. Sci. U.S.A. 90*, 6320−6324.
28. Doublié, S., Tabor, S., Long, A. M., Richardson, C. C., and Ellenberger, T. (1998) *Nature 391*, 251−258.
29. Kiefer, J. R., Mao, C., Braman, J. C., and Beese, L. S. (1998) *Nature 391*, 304−307.
30. Brautigam, C. A., and Steitz, T. A. (1998) *Curr. Opin. Struct. Biol. 8*, 54−63.
31. Kunkel, T. A., and Wilson, S. H. (1998) *Nat. Struct. Biol. 5*, 95−99.
32. Kohlstaedt, L. A., Wang, J., Friedman, J. M., Rice, P. A., and Steitz, T. A. (1992) *Science 256*, 1783−1790.
33. Wang, J., Smerdon, S. J., Jäger, J., Kohlstaedt, L. A., Rice, P. A., Friedman, J. M., and Steitz, T. A. (1994) *Proc. Natl. Acad. Sci. U.S.A. 91*, 7242−7246.
34. Dufour, E., el Dirani-Diab, R., Boulmé, F., Fournier, M., Nevinsky, G., Tarrago-Litvak, L., Litvak, S., and Andreola, M. L. (1998) *Eur. J. Biochem. 251*, 487−495.
35. Wlodawer, A., Miller, M., Jaskolski, M., Sathyanarayana, B. K., Baldwin, E., Weber, I. T., Selk, L. M., Clawson, L., Schneider, J., and Kent, S. B. (1989) *Science 245*, 616−621.
36. Dyda, F., Hickman, A. B., Jenkins, T. M., Engelman, A., Craigie, R., and Davies, D. R. (1994) *Science 266*, 1981−1986.

BI9731596